Available online at www.sciencedirect.com
SCIENCE DIRECT®
Journal of Power Sources 158 (2006) 169–176
JOURNAL OF POWER SOURCES
www.elsevier.com/locate/jpowsour

Performance of miniaturized direct methanol fuel cell (DMFC) devices using micropump for fuel delivery

Tao Zhang, Qing-Ming Wang *

Department of Mechanical Engineering, University of Pittsburgh, Pittsburgh, PA 15261, USA

Received 2 June 2005; accepted 25 June 2005
Available online 17 November 2005

Abstract

A fuel cell is a device that can convert chemical energy into electricity directly. Among various types of fuel cells, both polymer electrolyte membrane fuel cells (PEMFCs) and direct methanol fuel cells (DMFCs) can work at low temperature (<80 °C). Therefore, they can be used to supply power for commercial portable electronics such as laptop computers, digital cameras, PDAs and cell phones. The focus of this paper is to investigate the performance of a miniaturized DMFC device using a micropump to deliver fuel. The core of this micropump is a piezoelectric ring-type bending actuator and the associated nozzle/diffuser for directing fuel flow. Based on the experimental measurements, it is found that the performance of the fuel cell can be significantly improved if enough fuel flow is induced by the micropump at anode. Three factors may contribute to the performance enhancement including replenishment of methanol, decrease of diffusion resistance and removal of carbon dioxide. In comparison with conventional mini pumps, the size of the piezoelectric micropump is much smaller and the energy consumption is much lower. Thus, it is very viable and effective to use a piezoelectric valveless micropump for fuel delivery in miniaturized DMFC power systems.

Keywords: Direct methanol fuel cell; Piezoelectric valveless micropump; Fuel delivery; Experimental measurement

1. Introduction

Over the past few decades, there has been rapid technological developments in the area of portable electronic devices and systems. Numerous circuits, sensors, and actuators can now be fabricated on a single chip. However, the efficient power sources that are needed to drive these components or systems have not become correspondingly miniaturized. In many cases, frequent recharging is necessary to maintain the system's functionality. Hence, there is a need to design and fabricate a long-life, high-efficiency compact power system to provide the driving power for portable electronic systems. Of all the different types of power generation technologies, fuel cell technology that can convert the chemical energy of a reaction directly into electrical energy is particularly attractive due to its many advantages including high energy density, instant recharging, and low environmental impact [1–3].

Although there are a number of fuel cell technologies available for various applications, only those permitting near room-temperature operation are suitable for portable electronics. Therefore, polymer electrolyte membrane fuel cells (PEMFCs) and direct methanol fuel cells (DMFCs) that can work under 80 °C become the natural choice. Fuel choice is also very critical for commercial applications. Due to the storage, transportation and safety issues regarding hydrogen, fuel cells that directly use methanol as fuel have attracted a lot of research attention recently. Methanol has the highest energy to carbon ratio of any alcohol; it has a very high energy density (∼5 times that of hydrogen) and is environmentally friendly. All of these advantages make it an ideal choice for alternate fuel applications. The benefits and challenges in the development of DMFC have been discussed in details [4–7].

To realize the technical and economical advantages of DMFC, there are a number of issues that are critical and have not been fully resolved to date, such as methanol crossover, slow kinetics of DMFC reaction, and fuel delivery. Methanol crossover is the diffusion driven phenomenon of methanol traveling through the membrane from the anode side to the cathode. It lowers the efficiency of a DMFC in three key ways. First, the

* Corresponding author. Tel.: +1 412 624 4885; fax: +1 412 624 4846.
E-mail address: qmwang@engr.pitt.edu (Q.-M. Wang).

0378-7753/$ – see front matter
doi:10.1016/j.jpowsour.2005.06.043

methanol that crosses over is oxidized using energy that could have done work. Second, the phenomenon reduces the overall fuel efficiency by wasting fuel that could have been separated into protons and carbon dioxide. Lastly, the catalyst on the cathode side is easily poisoned by the presence of carbon atoms that stick to the catalyst and inactivate it. The other issue is the slow electrochemical reaction of DMFC. Previous research results have collectively led to the conclusion that the choice and preparation of the anode catalyst in a DMFC is far more important than in other types of fuel cells. This is because the kinetics of electro-oxidation of methanol at the anode is relatively slow, about six orders of magnitude lower than that of hydrogen near room temperature. Therefore, if the anode catalyst is of poor quality a DMFC may not even operate.

This research mainly focused on the fuel delivery problem in the miniaturized DMFC. A flow delivery system generally consists of pumps, valves, meters, and pipes, and its design and maintenance present virtually no critical technical issues on the macroscale fuel cell system. However, the situation is significantly different for a DMFC built for miniaturized or micro-scale power system operations. Inclusion of microfluidic devices, such as micropumps and microvalves would complicate the overall system, reduce reliability, and impose additional manufacturing costs. Also, the need for extra electrical power to drive the fuel delivery system could substantially penalize the overall performance the fuel cell system. The fuel delivery issue in miniaturized DMFC is further complicated by the presence of CO_2 gas as part of the reaction products in the vicinity of the anode. The accumulated CO_2 could form a barrier layer that prevents the replenished liquid methanol from reaching the anode. This, in turn, retards the reaction kinetics at the electrode and eventually degrades the entire fuel cell performance.

So far there are several different fuel delivery methods for miniaturized DMFC. One potential design is to drive the liquid fuel by gravitational and capillary forces [8]. This passive design did not consume extra power and the estimated fuel supply rate was adequate for acceptable performance. However, the structure design of the DMFC stack seemed to be very complicated and no experimental results of the actual fuel cell performance were reported. The other method is to choose an active pumping mechanism. In many experimental studies of miniaturized DMFC [9,10], a peristaltic pump was often used to supply methanol water solution. The flow rate was in the range of several ml min^{-1} and the size of the fuel cell was from several cm^2 to tens of cm^2. The actual performance of the fuel cell itself was acceptable but the extra power consumption of the pump was not considered. In this paper, a specifically designed micropump is utilized to drive fuel into a miniaturized DMFC and the performance of the whole system is investigated.

The piezoelectric valveless micropump used here for fuel delivery belongs to the category of reciprocating displacement micropumps. A piezoelectric bending actuator is used to drive the pump diaphragm oscillating periodically and inlet/outlet channels with suitable geometries rectify the fluid flow. This type of pump can provide a broad range of flow rates and pressure head with the minimum risk of valve wear, fatigue and clogging. One of the earliest piezoelectric valve-less micropumps was developed in 1993 [11]. In this micropump, conical nozzle/diffuser elements with small opening angles (<20°) were used to rectify the flow. Using water as working fluid, the maximum flow rate was 16 ml min^{-1} and the maximum pressure head was 2 m H_2O. Originating from this research, advanced designs with improved performance have been presented [12–16]. Other types of flow directing elements include pyramidic nozzle/diffuser elements with an opening angle of 70.5° [17,18] and valvular circuit [19,20].

In our previous paper [21], a compact design DMFC portable power system incorporating a piezoelectric valveless micropump has been presented. This design primarily includes a membrane electrolyte assembly (MEA), fuel flow chamber, fuel flow channel with nozzle/diffuser to control the flow direction, piezoelectric micropump for fuel delivery, and fuel supply manifold. The fuel supply manifold can be connected to an external methanol supply or a cartridge. By applying an alternating voltage, the pump actuator can drive the liquid methanol into the fuel cell system while expelling the CO_2 away from the vicinity of the anode. Theoretical analysis demonstrated that with an optimal system design, the piezoelectric micropump only consumed a very small amount of power generated by the fuel cell device while a satisfying cell performance was obtained. This paper is a continuing experimental study of the design aforementioned and the results are presented in the following sections.

2. Experimental setup

A piezoelectric valveless micropump prototype is fabricated in our lab. The material properties and dimensions of this prototype are listed in Table 1. Not all of the design parameters of the prototype are optimal due to the materials availability. To fabricate the thin PZT ring, first a PZT ring with a thickness of 0.8 mm is cut from a thicker PZT ring using the dicing saw, and then this PZT ring is grinded to the specific thickness. After that, the top and bottom surfaces of the PZT ring are coated with thin gold electrode layer using a sputter coater. The thin stainless steel disk is bought from McMaster-Carr Supply Company. The PZT ring is bonded onto the stainless steel disk using epoxy. Two very thin bare copper wires are connected to the two electrodes of this ring-type bonding actuator using conductive epoxy. The pump housing is made of hard transparent plastic material. By bonding the ring-type bending actuator onto the pump housing with epoxy, the valveless piezoelectric micropump is finally

Table 1
Dimensions and materials properties of the piezoelectric micropump actuator

	Piezoelectric ring	Bonding layer	Passive plate
Materials	PZT-5H	Conductive epoxy	Stainless steel
Inner diameter (mm)	6.3	6.3	
Outer diameter (mm)	19.11	19.11	25.4
Thickness (mm)	0.32	0.056	0.254
Young's modulus (Pa)	6.2×10^{10}	5.17×10^{9}	1.95×10^{11}
Poisson's ratio	0.31	0.3	0.3
d_{31} (m V^{-1})	-3.2×10^{-10}		
ε_{33}^{T} (F m^{-1})	2.856×10^{-8}		

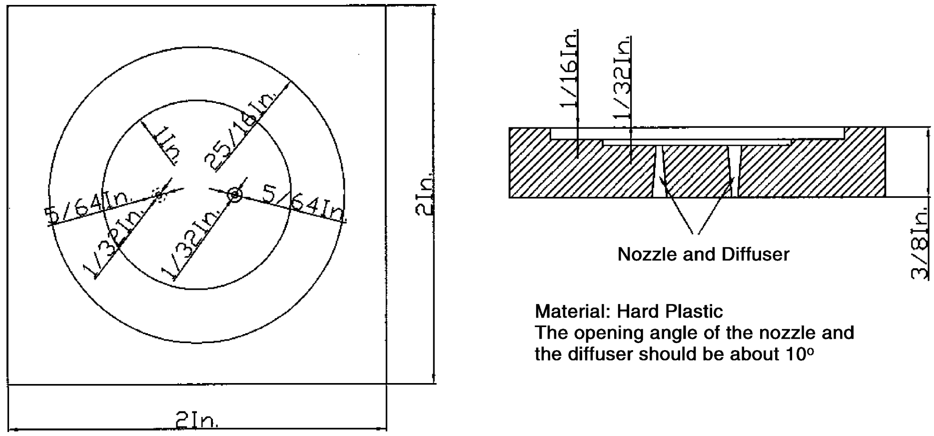

Fig. 1. Design graph of the micropump housing.

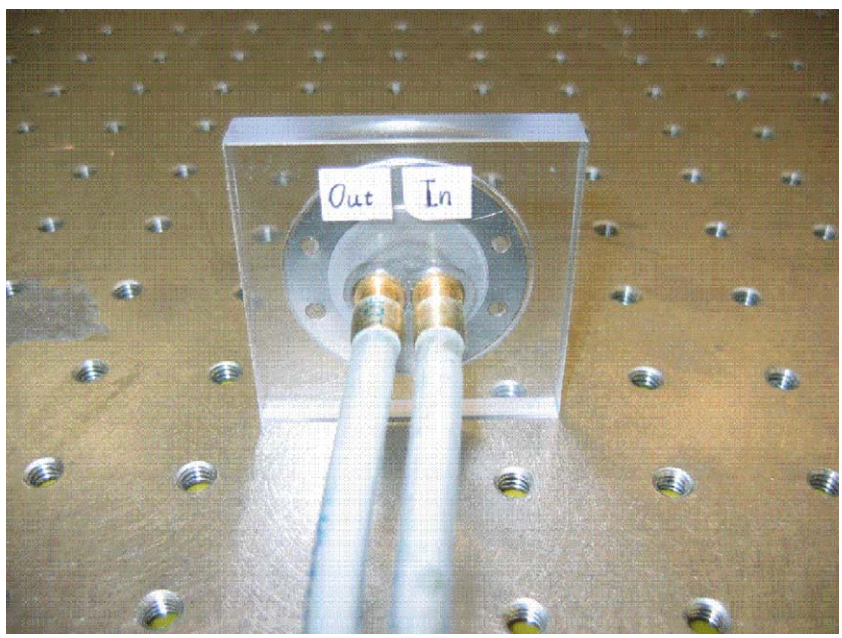

Fig. 2. Photo of the piezoelectric valveless micropump prototype.

assembled. The overall dimension of the micropump prototype is about 50 mm × 50 mm × 9 mm. Fig. 1 shows the top and cross section of the pump housing. Fig. 2 is the photo of this micropump prototype.

The experimental setup illustrated in Fig. 3 is used to characterize the performance of the micropump fabricated. A sinusoidal voltage signal is generated from a function generator (Stanford Research Systems Model DS345) and amplified through a power amplifier (AVC Instrumentation 790 Series). Then the amplified voltage signal is applied to the micropump actuator. A multimeter (FLUKE 45 Dual Display Multimeter) was used to monitor the applied voltage signal. The deflection of the micropump diaphragm was detected by a fiber optical detection system (MTI 2000 Fotonic Sensor). Another device that is not shown in the figure is an oscilloscope (Tektronix TDS 3032), which can measure the original voltage signal from the function generator and the response signal from the fiber optical sensor. To measure the water flow rate of this micropump, two water containers were connected to the inlet and outlet of the micropump separately. By measuring the movement the water surface inside the containers with respect to time, the average

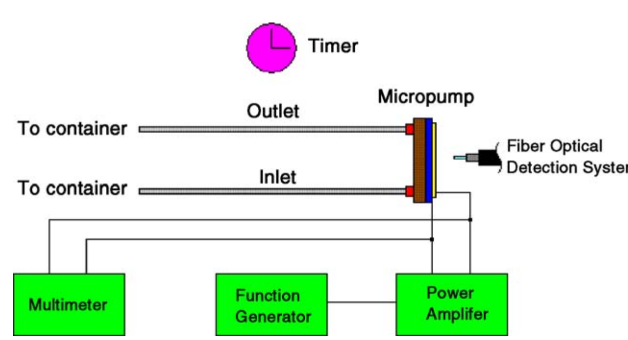

Fig. 3. Experimental setup for the micropump measurement.

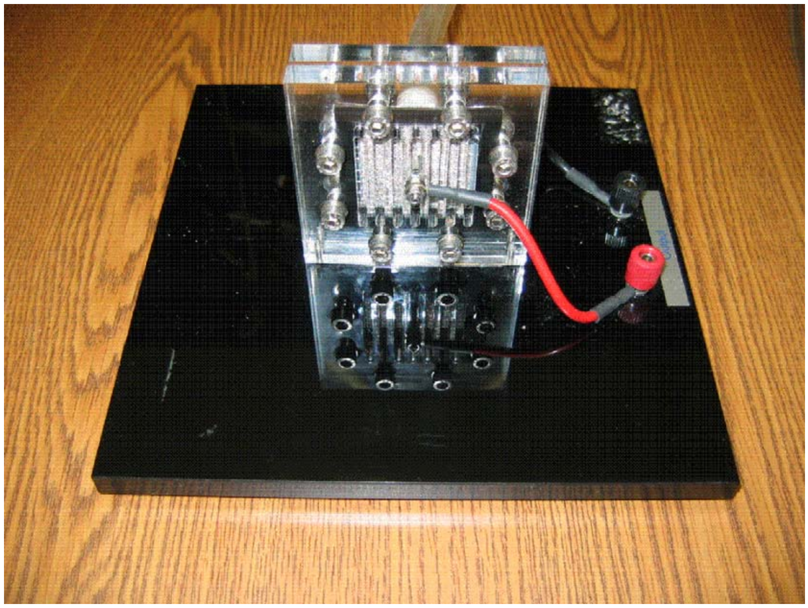

Fig. 4. Photo of the miniaturized DMFC device used in the experiments.

flow rate and the corresponding pressure head can be estimated. Furthermore, the impedance and the frequency response of the micropump was measured by connecting the two electrodes of the micropump actuator to an impedance analyzer (Agilent 4294A or Gamry Electrochemical Measurement System).

The experimental measurement of the performance of the miniaturized DMFC device (Fig. 4) driven by micropump has also been conducted. This fuel cell is made of a Nafion® membrane layer sandwiched by two electrode layers with catalysts deposited on them. The methanol water solution can be pumped into the anode side while the cathode side is exposed to air through a perforated plastic plate. The dimension of the fuel cell device is about 80 mm × 80 mm × 20 mm. To supply fuel to the fuel cell, the outlet of the micropump is connected to the anode of the DMFC device while the inlet of the micropump is connected to a tank filled with methanol water solution. By applying a sinusoidal voltage to the micropump actuator, a net fuel flow rate from inlet to outlet is obtained. The current output of the fuel cell can be controlled by A KEITHLEY 239 High Current Source Measure Unit precisely in the range of 0–1 A. And a FLUKE 45 Dual Display Multimeter is used to measure the voltage of the fuel cell.

3. Performance of the micropump

Since the micropump is specifically designed for driving methanol water solution as fuel for the DMFC power system, it is very important to investigate the pumping performance with liquid loading. Here, water is used as working fluid because its property is quite close to that of the methanol water solution. Concerning the self-priming capability and bubble tolerance, there exists a design criterion for the minimum compression ratio of a micropump [22]. During the fabrication of the micropump prototype, the thickness of the pump chamber is made as small as possible but the compression ratio is still much smaller than the theoretical criterion. To solve this problem, a commercial mini pump is used to fill the micropump with water and it turns out that the gas bubbles inside the pump chamber can be driven out quite easily.

As shown in Fig. 5, for the case with water loading, the relationship between the center deflection and the applied voltage is linear. This linear relationship was also predicted by the analytical analysis derived in our previous paper [21]. In this measurement, the applied voltage is sinusoidal and the driving frequency is 200 Hz. The frequency responses of the micropump with water loading are also evaluated by both center deflection measurement and actuator electric impedance spectrum measurement. From Fig. 6, it is found that the results obtained by both methods are very close and the resonance frequency is about 200 Hz. The results of the water flow rate measured under

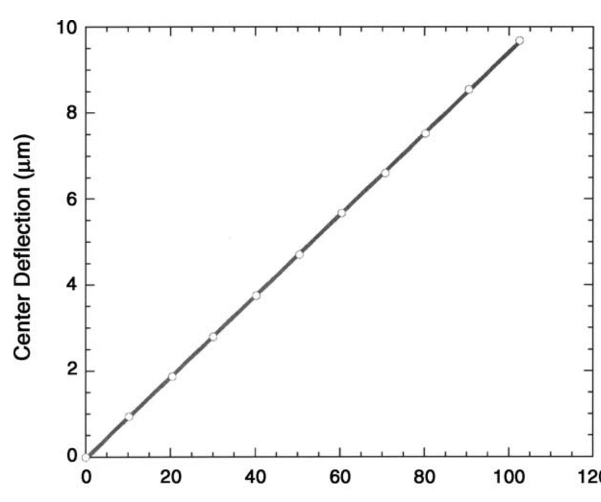

Fig. 5. Center deflection of the micropump diaphragm under different applied AC voltage (with water loading).

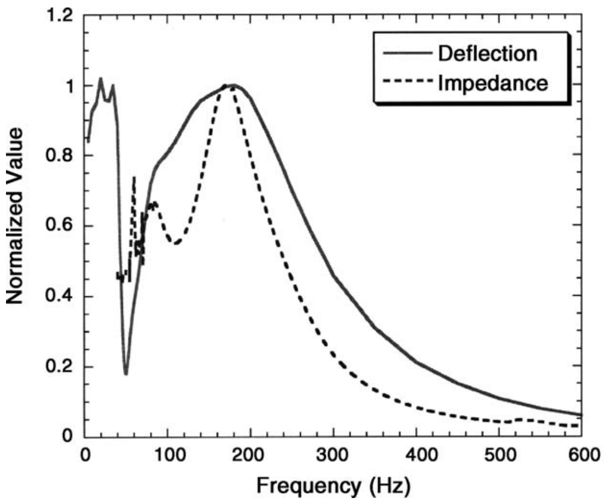

Fig. 6. Frequency response of the micropump obtained by different methods (with water loading).

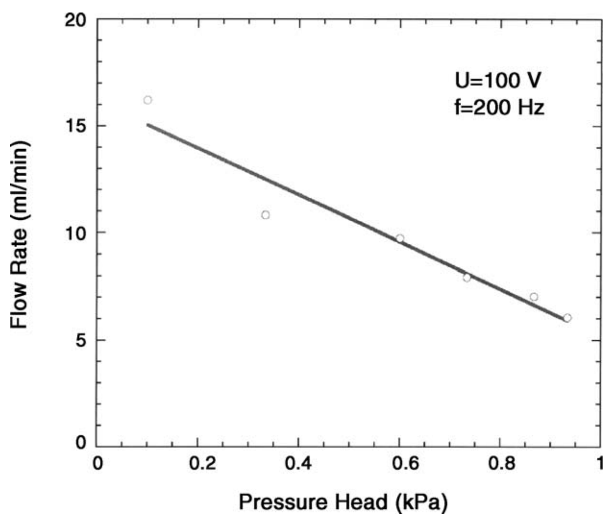

Fig. 7. Measured flow rate vs. pressure head (with water loading).

different pressure head are shown in Fig. 7. The larger flow rate corresponds to the lower pressure head. Using this micropump, a flow rate of 5 ml min^{-1} at 1 kPa can be delivered when applying a 100 V voltage with a driving frequency of 200 Hz. The maximum value of the measured capacitance is about 8.22 nF and it can be estimated that the maximum power consumption is around 50 mW.

4. Performance of the DMFC device with and without pump

For comparison, the characteristic curves of the DMFC devices are measured at room temperature using a different concentration of methanol water solution as fuel and no pump is used. Under this circumstance, the fuel is simply fed by gravitational force and diffusion. Since the cathode side of this DMFC device is a complicated multilayer structure with small perforated holes, it is difficult to estimate the exact effective area for electrochemical reaction (about several cm^2) and the exact current density. Therefore the *x*-coordinate of the figure is not current density but current. As shown in Fig. 8, three different concentrations of methanol water solution are used: 0.2, 1 and 2 M. The open circuit voltage (OCV) of three cases is between 0.6 and 0.7 V. Using the Nernst equation, the ideal cell potential of the DMFC is about 1.21 V under our experimental conditions. Therefore, the potential loss in this case is quite high. Some of the loss may be caused by methanol crossover [23] and others may be induced by the existence of a very small leakage current [24]. More detailed research is required to verify these losses. It is also observed that at low cell current, the performance doesn't vary too much. But at medium and high cell current, the difference is very significant. The higher the concentration is, the better the cell performance. The fuel cell power is calculated by multiplying the cell voltage with the cell current and the results are shown in Fig. 9. Note that the maximum power obtained using 1 M methanol is very close to the maximum power obtained using 2 M methanol although the maximum applicable currents

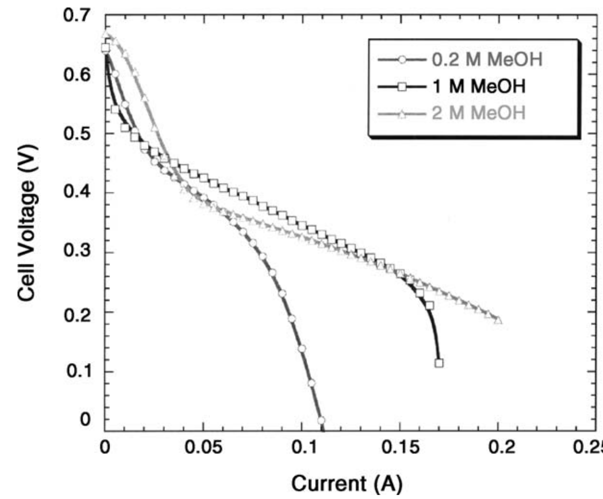

Fig. 8. Measured characteristic curves of the DMFC device using different concentration of methanol water solution.

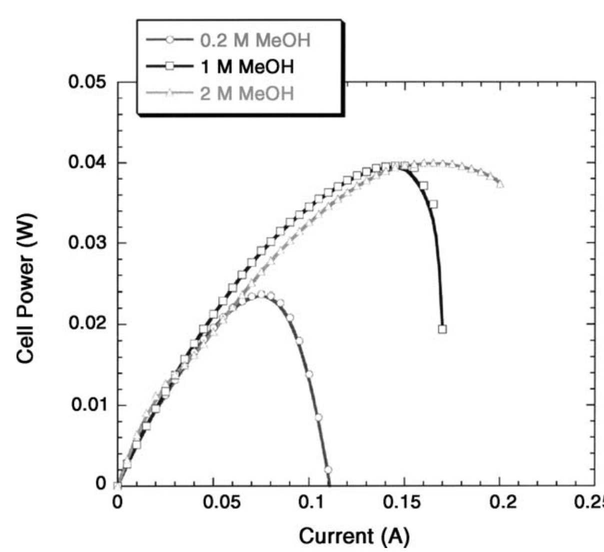

Fig. 9. Calculated power of the DMFC device using different concentration of methanol water solution.

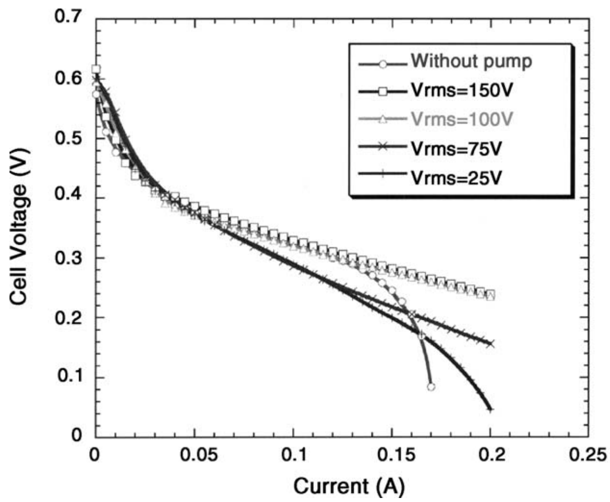

Fig. 10. Measured characteristic curves of the DMFC device driven by micropump.

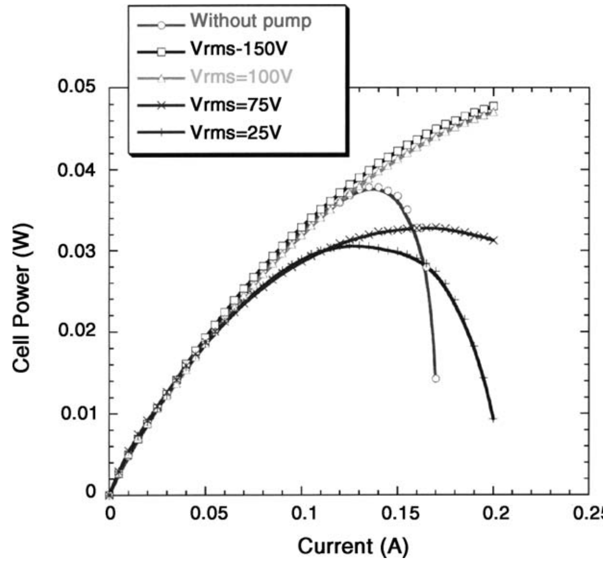

Fig. 11. Calculated power of the DMFC device driven by micropump.

of two cases are different. The steep performance drop appearing at the relatively large current is often caused by diffusion loss. In the following experiments, the fuel concentration is fixed at 1 M and the fuel cell performance with the use of micropump is evaluated.

The micropump prototype fabricated in our lab can be connected to the DMFC device to provide a fuel flow rate and the performance of this combined system is measured. The flow rate of the micropump is controlled by the driving voltage. Higher driving voltage corresponds to higher flow rate. As shown in Fig. 10, four different driving voltages are used: 150, 100, 75 and 25 V. Based on Fig. 7, the cell power can be calculated and the results are shown in Fig. 11. For comparison, the characteristic curve of the fuel cell using 1 M methanol without pump is also added in the figure. All of the data are measured under room temperature. The OCV of all the curves are close to 0.6 V so the potential loss at zero current doesn't change too much with fuel flow rate. When the current is small, the difference between each curve is not significant. When the current is increasing, the voltage of the fuel cell with lower fuel flow rate is dropping more quickly except for the case with zero fuel flow rate (no pumping). It is also observed that the performances at driving voltage of both 100 and 150 V are very close and much better than the performance without the pump. However, the performances at driving voltage of both 75 and 25 V are somehow worse than the performance without the pump. This performance deterioration is not expected from the analytical analysis and the reason for it has to be examined in future research. In conclusion, the

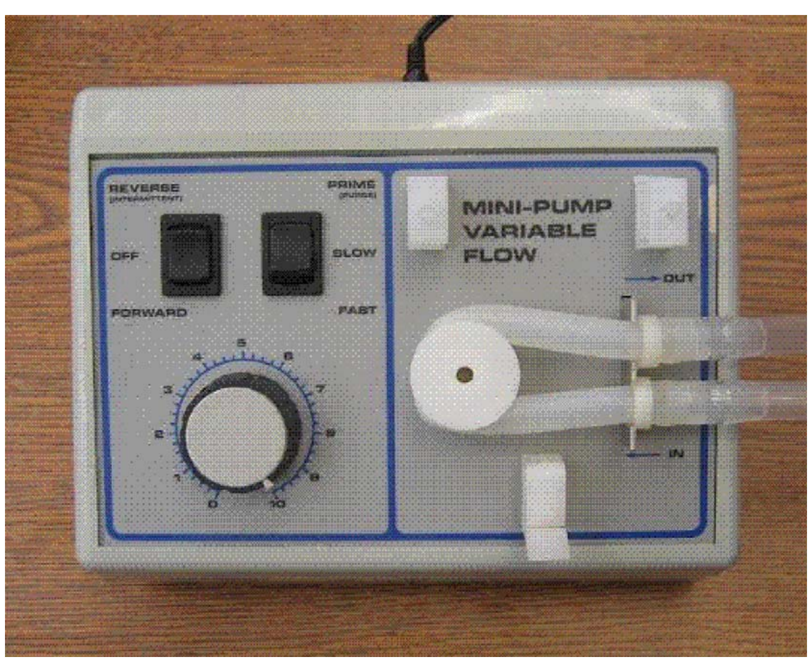

Fig. 12. Photo of the peristaltic variable flow mini pump.

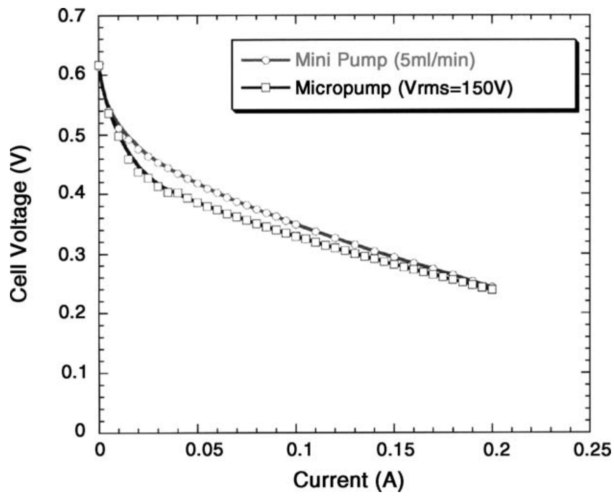

Fig. 13. Comparison of the characteristic curves between using micropump and using mini pump.

enhancement of the fuel cell performance by using a micropump has been observed and the detailed reasons will be discussed later.

A peristaltic mini pump shown in Fig. 12 is also used to supply fuel to the fuel cell device and the performance of it can be compared with that of the micropump. The original usage of this mini pump is to fill the micropump prototype with liquid and drive the air out of it. The flow rate of the mini pump is variable between 0.03 and 8.2 ml min^{-1}. The dimension of mini pump is 168 mm × 120 mm × 115 mm. The results of the comparison between the fuel cell performance using the micropump and the fuel cell performance using the mini pump are shown in Figs. 13 and 14. All the tests were at room temperature. The flow rate of the mini pump was kept at 5 ml min^{-1}. As for the micropump, the driving voltage was 150 V and the driving frequency was 200 Hz. It is found that the performance using the mini pump is only slightly better than the performance using the micropump. And both of them are much better than the performance without a pump. With almost the same performance as

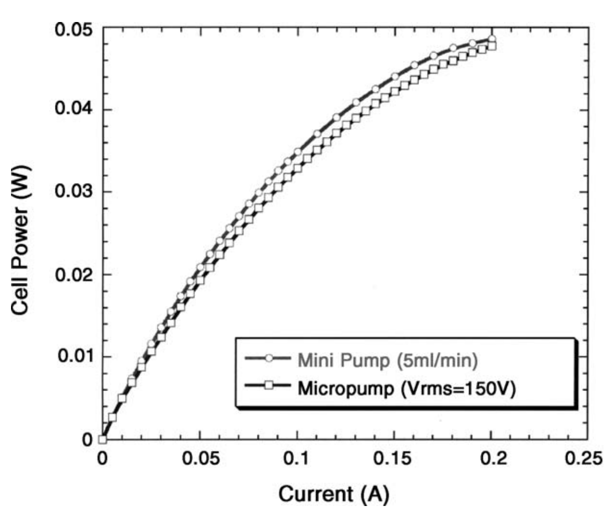

Fig. 14. Comparison of the cell power between using micropump and using mini pump.

the mini pump, the size of the micropump is much smaller and the power consumption is much lower. It is estimated that the power consumption of the mini pump is about several watts, too large for portable power applications. The capacitance of the micropump actuator is about 8.22 nF. Driving by a sinusoidal voltage of 150 V at 200 Hz, the maximum power consumption of the micropump is about 116 mW based on previous analysis. Therefore, the micropump is applicable for the portable power applications ranging from 1 to 50 W. Moreover the micropump can be easily integrated with the planar structure of fuel cell and the whole power system can be very compact.

5. Analysis and discussion

Based on the experimental data, it is concluded that the performance of the DMFC can be improved by adding a forced flow through the anode by incorporating a micropump into the fuel cell system. The reasons for this may include avoidance of the fuel depletion, decrease of diffusion resistance, and removal of carbon dioxide. During the operation of the DMFC, methanol is consumed by the electrochemical reaction along the anode side and the concentration diminishes. A forced fuel flow can circulate the fuel and provide fresh fuel to the reaction sites. Also in fuel cell reactions, the concentration of the bulk solution and concentration of the solution at the anode interface are different. The methanol needs to diffuse from the bulk solution to the anode/catalyst interface and the carbon dioxide has to migrate back to the bulk. In this process, diffusion resistance exists and the disturbance of the bulk solution due to the pumping can minimize this resistance.

The last factor, the removal of carbon dioxide is also very important to the performance of the DMFC. When the current is along the surface of the anode, the carbon dioxide will be generated at the same time. The size of the carbon dioxide bubbles will continue to grow if they are not removed from the anode surface. So when the reaction continues, more surfaces will be occupied by carbon dioxide bubbles and the performance will deteriorate. A forced fuel flow can carry these carbon dioxide bubbles away when the size of them is still small. There exists a relationship between the flow rate and the size of the gas bubbles that can be removed with the flow. By calculating the buoyancy force of the gas bubble and the drag force by the fluid, some theoretical model can be developed to describe this problem. In our experiments, the anode side of the DMFC devices is covered with a transparent glass plate therefore the formation of the carbon dioxide bubbles can be visually observed. For the operations without pump, there are a lot of gas bubbles clinging to the anode surface when the current density is high or the operation time is long. With the help of pumping, majority of the bubbles can be effectively removed and the accumulation of the bubbles at the anode surface is stable. Therefore, the performance is improved.

6. Summary

In this paper, the experimental study of a miniaturized DMFC device using piezoelectric valveless micropump for fuel delivery is presented. It is found that driving by a 100 V voltage at 200 Hz, the micropump prototype can supply a 5-ml min^{-1} of water flow rate at 1 kPa. The performance of a miniaturized DMFC device can be improved by using this micropump to supply methanol fuel.

Acknowledgments

The authors would like to acknowledge the financial support from the Pittsburgh Digital Greenhouse, a strategic economic development initiative with research and development focus on System-on-Chip (SoC) and related technologies for networking and multimedia applications. This work is also partially supported by University of Pittsburgh Small Grant Funding.

References

[1] C. Hebling, A. Heinzel, U. Groos, Technology and Markets for Portable Fuel Cells, Seventh Grove Fuel Cell Symposium, London, UK, 2001.
[2] A. Heinzel, C. Hebling, M. Müller, M. Zedda, C. Müller, J. Power Sources 105 (2002) 250–255.
[3] C.K. Dyer, J. Power Sources 106 (2002) 31–34.
[4] S. Gottesfeld, Direct Methanol Fuel Cells for Portable Power, Fuel Cell Portable Power Workshop, Phoenix, USA, January 15–17, 2002.
[5] R. Dillon, S. Srinivasan, A.S. Aricò, V. Antonucci, J. Power Sources 127 (2004) 112–126.
[6] V. Gogel, T. Frey, Z. Yongsheng, K.A. Friedrich, L Jörissen, J. Garche, J. Power Sources 127 (2004) 172–180.
[7] A. Oedegaard, C. Hebling, A. Schmitz, S. Møller-Holst, R. Tunold, J. Power Sources 127 (2004) 187–196.
[8] M.M. Mench, Z.H. Wang, K. Bhatia, C.Y. Yang, Design of a micro direct methanol fuel cell (μDMFC), International Mechanical Engineering Congress and Exposition (IMECE), New York, USA, November 11–16, 2001.
[9] A.K. Shukla, P.A. Christensen, A.J. Dickinson, A. Hamnett, J. Power Sources 76 (1998) 54–59.
[10] K. Scott, P. Argyropoulos, P. Yiannopoulos, W.M. Taama, J. Appl. Electrochem. 31 (2001) 823–832.
[11] E. Stemme, G. Stemme, Sens. Actuat. A 39 (1993) 159–167.
[12] A. Olsson, G. Stemme, E. Stemme, Sens. Actuat. A 46–47 (1995) 549–556.
[13] A. Olsson, G. Stemme, E. Stemme, Sens. Actuat. A 57 (1996) 137–143.
[14] A. Olsson, P. Enoksson, G. Stemme, E. Stemme, J. Micromech. Microeng. 6 (1996) 87–91.
[15] A. Olsson, P. Enoksson, G. Stemme, E. Stemme, J. Microelectromech. Syst. 6 (No. 2) (1997) 161–166.
[16] A. Olsson, PhD Thesis: Valve-less Diffuser Micropumps, Royal Institute of Technology, Stockholm, Sweden, 1998.
[17] T. Gerlach, M. Schuenemann, Helmut Wurmus, J. Micromech. Microeng. 5 (1995) 199–201.
[18] T. Gerlach, H. Wurmus, Sens. Actuat. A 50 (1995) 135–140.
[19] F.K. Forster, R.L. Bardell, M.A. Afromowitz, N.R. Sharma, A. Blanchard, Proceedings of the ASME Fluids Engineering Division, FED-Vol. 234 (1995) 39–44.
[20] R.L. Bardell, N.R. Sharma, F.K. Forster, M.A. Afromowitz, R.J. Penney, Microelectromechanical Systems (MEMS) ASME, DSC-Vol. 62/HTD-Vol. 354 (1997) 47–53.
[21] T. Zhang, Q.-M. Wang, J. Power Sources 140 (2005) 72–80.
[22] M. Richter, R. Linnemann, P. Woias, Sens. Actuat. A 68 (1998) 480–486.
[23] V.M. Barrageán, A. Heinzel, J. Power Sources 104 (2002) 66–72.
[24] B. Gurau, E.S. Smotkin, J. Power Sources 112 (2002) 339–352.